PAPER Special Section on Image Media Quality

Evaluation of Image Corrected by Retinex Method Based on S-CIELAB and Gazing Information

Jie BAI[†a)], *Member*, Toshiya NAKAGUCHI[†], *Member*, Norimichi TSUMURA[†], *Member*, and Yoichi MIYAKE[††], *Member*

Summary
The purpose of this research is to propose an effective color metric which can predict the perceptual image quality for Retinex method. In this paper, we first give a brief introduction of three kinds of typical single Retinex methods to improve the color reproduction. And then, we state the process for obtaining the observer rating value from the subjective evaluation experiment performed under the sRGB illumination condition. Next, we introduce the S-CIELAB metric and propose a new metric on the basis of S-CIELAB metric that considers the gazing information. The average S-CIELAB color differences with and without the consideration of gazing information were calculated as the objective image quality measures. The correlations between the observer rating values and the objective image quality measures were calculated. The result shows that all of the average S-CIELAB color differences based on the gazing information are better correlated to the observer rating value than the average S-CIELAB color difference over the whole area. The average S-CIELAB color difference weighted by the gazing frequency over the gazing area shows the strong correlation with the observer rating value.

Key words:
Retinex method, S-CIELAB metric, gazing frequency, gazing area

1. Introduction

The increased availability of color imaging systems, computer power and broadband network has changed all of our life as a multi media age. In the multi media age, many kinds of color images have been widely used for e-commerce, medicine, recording, printing and so on. In this process, it is always required to reproduce natural color and tone corrections of the image by using many image processing methods, such as tone mapping, gamma correction, gamut mapping, histogram transformation, Retinex processing and so on. The parameters are adjusted by the perceptions of the observers with skill to the most suitable image. Thus the standard methods for image quality measurement must necessarily rely on the psychophysical experimentation. However, the psychophysical experiments are very time consuming and expensive to complete properly [1]. Therefore, an effective metric which can predict the perceptual image quality for these image processing methods is expected.

In this research, we concentrate on Retinex method. Retinex method is based on Land's Retinex model for lightness and color constancy of the human eye [2]. It has been applied to image processing for color correction because it can improve the image quality of the underexposure image, the backlight image, and the image taken under some illuminant that with a little color, such as the standard illuminant A. The image quality of these images can not be improved very well by using the conventional image processing methods, such as histogram equalization, linear operation, and so on. Multi-Scale Retinex has been reported more effective than Single-Scale Retinex [3], the selection of the parameter in it, such as the size of the scale, is very important to decide the final reproduced color image quality. However, it is not easy to decide this parameter. And until now, for Retinex method, quality criteria method well correlated to the evaluation by those observers are not defined. Therefore, in this research, the purpose is to propose an effective color metric which can predict the perceptual color image quality for Retinex method. We used the proposed metric to predict the change of the perceptual color image quality of the produced resultant images by using the Single-Scale Retinex method with different scales whose size is different. And it is expected to be used as the quality criteria of the parameter selection in the automatic image processing system in the near future.

The traditional color metric approach to color image quality is to measure the color differences of large uniform patches between the reproduction and the original (or others decided according to the purpose). The results are then typically expressed in terms of average color differences or with histograms of color differences. The metrics utilized include the CIELAB ΔE^*_{ab} Euclidean color difference formula, the CIE94 color difference equation that corrects first-order non-uniformities in the CIELAB [4]. Another color metric approach is the S-CIELAB [5] color metric, which is a spatial extension to

[†]The authors are with Graduate School of Science and Technology, Chiba University, 1-33 Yayoi-cho, Inage-ku, Chiba-shi, 263-8522, Japan
[††]The author is with Research Center for Frontier Medical Engineering, Chiba University, 1-33 Yayoi-cho, Inage-ku, Chiba-shi, 263-8522, Japan
a) E-mail: baijie@graduate.chiba-u.jp

the CIELAB color metric that is useful for measuring color reproduction errors of digital images. Both CIELAB and S-CIELAB are the color difference metrics calculated over the whole area. It is well known that an image has a particular gazing area [6], and in the experimental results and our previous papers [7-9], we found that the total image quality is highly influenced by the gazing area. Miyata *et.al* [7] had verified the physical quality criterion within the gazing area is well correlated to the observer rating value. However, they only discussed the sharpness and the graininess characteristics of the observed images. And, they considered neither 2-degree visual field of the human eye nor the spatial change within the gazing area when they analyzed the gazing information. Therefore, in this research, we propose a new color metric based on S-CIELAB metric with the consideration of gazing information for Retinex method. The gazing information includes both the gazing area considering 2-degree visual field and the gazing frequency within the gazing area. Finally, the effectiveness of the proposed metric is discussed.

2. Retinex Methods

Three kinds of typical single Retinex methods are considered in this research; the standard non-linear Retinex method (NLR) [10], the extended version of the non-linear Retinex method (ENLR) [11], and the linear Retinex method (LR) [12]. In the ENLR, the original pixel value is adaptively introduced into the output to keep the color balance. Each method has its own advantages and drawbacks respectively.

2.1 Non-Linear Retinex Method (NLR)

In the standard non-linear Retinex method, the Retinex output is given by

$$R_i(x,y,\sigma_{i,m}) = \log\left(\frac{I_i(x,y)}{I_i(x,y)\otimes F_{i,m}(x,y)}\right) \quad (1)$$

where, $I_i(x,y)$ is the image distribution in the ith spectral band, in this research, $i = r, g, b$. The symbol " $\otimes$ " denotes the convolution operation, m is the size of the radius of the scale, and $F_{i,m}$ is the surround function for the scale m

$$F_{i,m}(x,y) = K \times \exp\left[-\left(x^2+y^2\right)/\sigma_{i,m}{}^2\right] \quad (2)$$

where, the standard deviation $\sigma_{i,m}$ is the Gaussian surround space constant. And K is selected such that

$$\iint F_{i,m}(x,y)dxdy = 1 . \quad (3)$$

2.2 Extended Non-Linear Retinex Method (ENLR)

The ENLR is based on the standard Retinex method. It can be expressed as

$$R_i(x,y,\sigma_{i,m}) = d \times \log\left(\frac{I_i(x,y)}{I_i(x,y)\otimes F_{i,m}(x,y)}\right) + (1-d)\times I_i(x,y) \quad (4)$$

where, d is a ratio of the resultant image by the standard Retinex method to the original image. In this method, the original pixel value I_i is adaptively introduced into the output to keep the color fidelity.

2.3 Linear Retinex Method (LR)

The linear Retinex with no *logarithm* processing is simply described by

$$R_i(x,y,\sigma_{i,m}) = A(\sigma_{i,m}) \times \frac{I_i(x,y)}{S_{i,m}(x,y,\sigma_{i,m})} \quad (5)$$

where, $S_{i,m}$ is the surround function for the scale m in the luminance Y space which is given by

$$S_{i,m}(x,y,\sigma_{i,m}) = F_{i,m}(x,y)\otimes Y(x,y) \quad (6)$$

and the gain function $A(\sigma_{i,m})$ designed based on the Center/Surround histogram is expressed as

$$A(\sigma_{i,m}) = M\left\{\sum\nolimits_{C/S}(\sigma_{i,\mathrm{m}}) \Big/ \sum_{\mathrm{m}=1}^{\mathrm{M}} \sum\nolimits_{C/S}(\sigma_{i,\mathrm{m}})\right\} \quad (7)$$

where

$$\sum\nolimits_{C/S}(\sigma_{i,m}) = \sqrt{\frac{1}{XY}\sum_{x=1}^{X}\sum_{y=1}^{Y}\left[Y_{C/S}(x,y,\sigma_{i,m}) - Ave\{Y_{C/S}(x,y,\sigma_{i,m})\}\right]^2} \quad (8)$$

and

$$Y_{C/S}(x,y,\sigma_{i,m}) = Y(x,y)/S_{i,m}(x,y,\sigma_{i,m}) \quad (9)$$

and the capital letter M is the number of the scale.

For all of the above Retinex methods, a single gain-offset was selected which actually clips both the highest and lowest signal transitions before transporting the output to the display.

To avoid the influence from the non-linear characteristic of the capturing system, the gamma of the test images added by the capturing system was corrected. After the processing the gamma was added in the LR. In contrast, in two non-linear Retinex methods, NLR and ENLR, the *logarithm* processing plays a role of adding gamma onto the output; therefore, the clipped value was directly transported to the display.

3. Subjective Evaluation Experiment

3.1 Test Images

(a) Image taken under standard illuminant A (b) Underexposure image

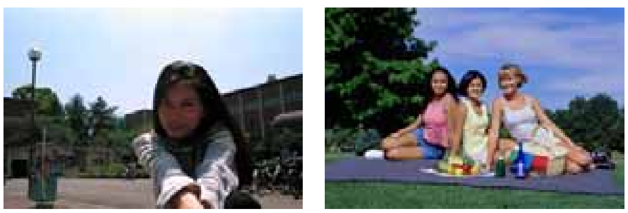

(c) Backlight image (d) Image taken under correct exposure

Fig.1 Test images used in the subjective evaluation experiment. They are (a) an image taken under standard illuminant A; (b) an underexposure image; (c) a backlight image; (d) an image taken under correct exposure.

Four kinds of test images (450×300, and 300×450 pixels at 8 bits) used in this research are shown in Fig.1. They are an image taken under standard illuminant A (from the standard spectral image database), an underexposure image (taken by using D1X, Nikon *Corp.)*, a backlight image (color negative film scanned by film scanner), and an image taken under correct exposure (Sony sRGB standard image), respectively. These images were selected in consideration of the characteristic of Retinex method.

Test images for the subjective evaluation experiment were produced by changing the size of the radius of the scale, *m*, in each Retinex method. Therefore, twelve groups of images were produced for the evaluation of image quality. The same value *m* is selected for each spectral band. To ensure the subjective visual quality increases with the size of the scale monotonously, we selected the scales as follows. For the NLR and the ENLR, m = 90, 120, 180, 260 pixels. For the LR, m = 70, 90, 120, 180 pixels.

Figure.2 shows the example images produced by using the ENLR for the subjective evaluation experiment of Fig.1 (a) and (c). In Fig.2 (a), the color shift caused by

(1) m = 90 (2) m = 120 (3) m = 180 (4) m = 260 (pixels)

(a) Resultant images of the image taken under standard illuminant A

(1) m = 90 (pixels) (2) m = 120 (pixels)

(3) m = 180 (pixels) (4) m = 260 (pixels)

(b) Resultant images of the backlight image

Fig.2 Two groups of resultant images used in the subjective evaluation experiment produced by using the ENLR with different scales whose size is different. The sizes of the radius of the scale of these images are (1) m=90; (2) m=120; (3) m=180; (4) m=260 pixels, respectively.

standard illuminant A is corrected. In Fig.2 (b), the shadow on the face of the woman caused by backlight is removed. As shown in Fig.2, the whole appearances of the resultant images by using different scales are very similar except some striking differences such as the place just before the left bottle in Fig.2 (a) and so on. It is verified in the following section that these places are frequently gazed, and they gave strong influences to the subjective judgments of the observers.

3.2 Subjective Evaluation Experiment

In the subjective evaluation experiment, images were evaluated on BARCO CRT display with high accuracy color reproduction characteristic by using the paired-comparison method under the standard sRGB illumination condition. At a viewing distance of 50 cm, the observers were asked to select the image shows more natural color in total image quality from two images presented on the display. Subjective image quality was collected and analyzed across sixteen observers who are students with normal sense of color and visual acuity in our laboratory (thirteen males, three females). The psychophysical distance was calculated following the assumption of the Thurstone's case V. The normalized psychophysical distance is used as the observer rating value in our research. The correlation between the observer rating value and the calculated objective image quality measure is discussed in section 6.

4. Measurement of Gazing Information

4.1 Eye Tracking Instrumentation

The eye tracking system (EMR-NL8B, Nac Image Technology Inc) was used in the subjective evaluation experiment. The main components of this system include an eyeball photography camera which houses an infrared LED illuminator and an eye camera, a controller, a LED power supply box, a signal conversion box, and a chin level. Eye movement is detected by calculating the distance between the image of purple and the reflected image of an infrared LED illuminator on the cornea.

4.2 Measurement and Analysis of the Gazing Information

Eye movements of sixteen observers during the viewing of the images in the subjective evaluation experiment were measured. Eye tracking recordings from six of the sixteen observers were discarded due to poor calibration, excessive number of track losses, and problems related to equipment failure.

Because the system is based on NTSC video signals, sight point is calculated at 60 Hz (video rate). The eye mark analyzing software allows for variable field averaging reducing signal noise. Gazing point (x, y) is obtained from the sight points over 8 video fields, which yields an effective temporal resolution of 133 msec [13], in the way described as follows. If the distance between the initial two sight points is within a certain scope, the two sight points belong to the same group. From the initial two sight points, the first center of gravity (COG) of the initial two sight points can be obtained. In the same way, if the distance between the first COG and the third sight point is within the same scope, the three sight points belong to the same group. The second COG which is the COG of the first COG and the third sight point can be obtained. In this research, we let the scope be 2-degree visual field. For such consecutive $n(n > 8)$ sight points

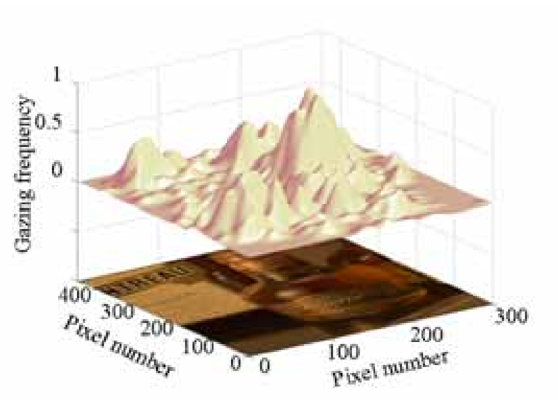

(a-1) In case of the used images in the subjective evaluation experiment is produced by using NLR

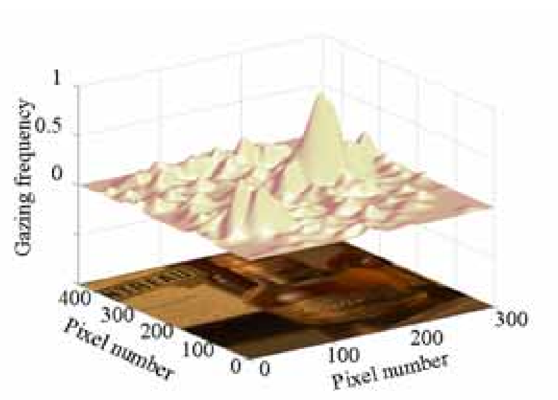

(a-2) In case of the used images in the subjective evaluation experiment is produced by using ENLR.

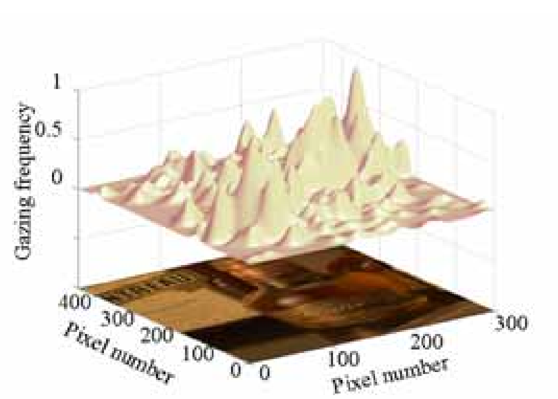

(a-3) In case of the used images in the subjective evaluation experiment is produced by using LR

(a) Results by using the image taken under standard illuminant A

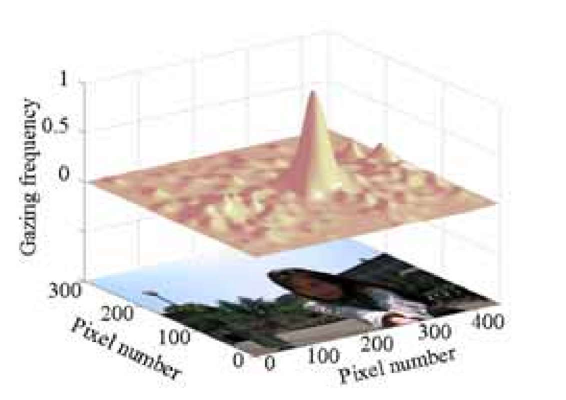

(b-1) In case of the used images in the subjective evaluation experiment is produced by using NLR

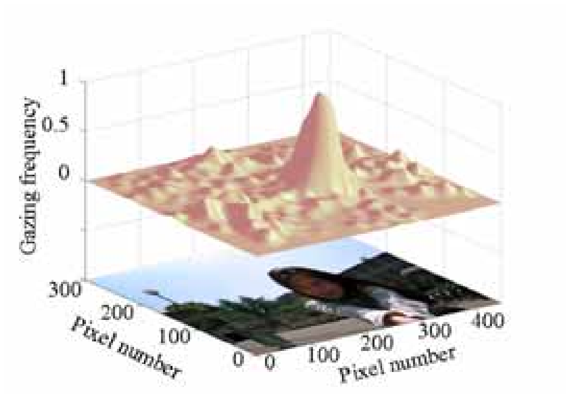

(b-2) In case of the used images in the subjective evaluation experiment is produced by using ENLR

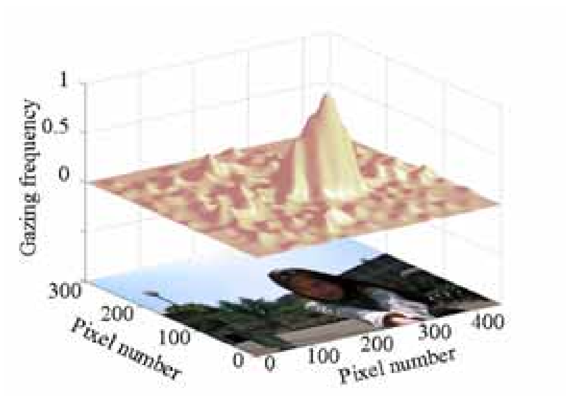

(b-3) In case of the used images in the subjective evaluation experiment is produced by using LR

(b) Results by using the backlight image

Fig.3 The normalized gazing frequency map in consideration of 2-degree visual field of the human eye across ten observers

(a) Results by using the image taken under standard illuminant A

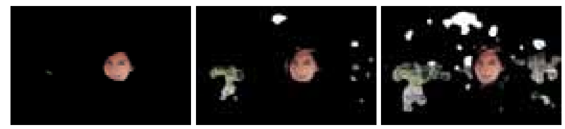

(b) Results by using the backlight image

Fig.4 Gazing areas obtained with different threshold. From the left to the right, the thresholds are 0.2, 0.1, and 0.05 respectively. (The resultant images are the ones produced by the ENLR with a Gaussian scale whose radius is 90 pixels.)

belonging to the same group, $(n-1)$ COG can be obtained. The $(n-1)th$ COG is defined as gazing point (x,y) [14].

4.3 Gazing Frequency Map

Gazing frequency map is an index that shows the gazed degree. At each gazing point (x,y), the normalized spatial gazing frequency $F(x,y)$ is calculated by

$$F(x,y) = \left\{ \frac{T(x,y)}{N(x,y)} \right\}_{nol} \qquad F(x,y) \in [0,1] \tag{10}$$

where, $T(x,y)$ and $N(x,y)$ denote the total gazing time and the number of times of gaze, respectively. The subscript *nol* means normalization. Furthermore, from the physiologic viewpoint, when a person observes an object, not only one point, but also its surrounding is seen simultaneously. The scope including the point and its surrounding is called visual field. In this field, the obtained information decreases if apart from the eye beam [14]. We consider this characteristic of the human eye by convolving the obtained frequency with a Gaussian filter corresponding to the 2-degree visual field of the human eye [13]. In this way, a gazing frequency map with consideration of the 2-degree visual field of the human eye $F'(x,y)$ can be obtained. In this research, the integral value of the Gaussian filter is defined to be one.

Figure.3 shows the normalized gazing frequency maps with the consideration of 2-degree visual field of the human eye, the higher the gazing frequency of an area is, the more frequently the area is gazed at.

4.4 Gazing Area

The gazing area $G(x,y)$ is obtained from the gazing frequency map with the consideration of 2-degree visual field of the human eye $F'(x,y)$, it is defined by

$$G(x,y)=\begin{cases}1 & F'(x,y)>\theta \\ 0 & F'(x,y)<\theta\end{cases} \quad (11)$$

where, the threshold θ is within [0, 1]. Figure.4 shows the images covered by the extracted gazing area with different threshold. They are 0.2, 0.1, and 0.05, respectively.

5. Color metric

Each Retinex method has its own advantages and drawbacks respectively, and it is also difficult to set the parameters of the methods to all sample images. To adjust the parameters of Retinex method empirically, it takes much effort and time. Therefore, an effective metric which can predict the perceptual image quality for Retinex method is expected.

In this research, we propose a new color metric based on the S-CIELAB color metric with the consideration of gazing information.

5.1 S-CIELAB Metric

S-CIELAB metric is a spatial extension to the CIELAB color metric that is useful for measuring color reproduction errors of digital images [5]. Figure.5 shows a flow chart for showing how to calculate the S-CIELAB error map.

As shown in Fig.5, the image data are transformed into the opponent-color space, which has w/k, r/g, and b/y color dimensions. Each opponent-color image is convolved with a scale whose shape is determined by the visual spatial sensitivity to that color dimension. Finally, the filtered representation is transformed using the CIELAB formulae to calculate the S-CIELAB error map.

In this research, for each Retinex method and for each image, the S-CIELAB color difference between the resultant images by using the smallest scale and the one by using any scale in the same group was calculated pixel-to-pixel. For one group of image, four average S-CIELAB color differences could be calculated. The objective image quality measure $Q_{S-CIELAB}$ was obtained by normalizing these average S-CIELAB color differences by the maximum S-CIELAB color difference in the group.

5.2 S-CIELAB Metric in Consideration of Gazing Information

In this research, we also considered the gazing information. The average S-CIELAB color difference weighted by the

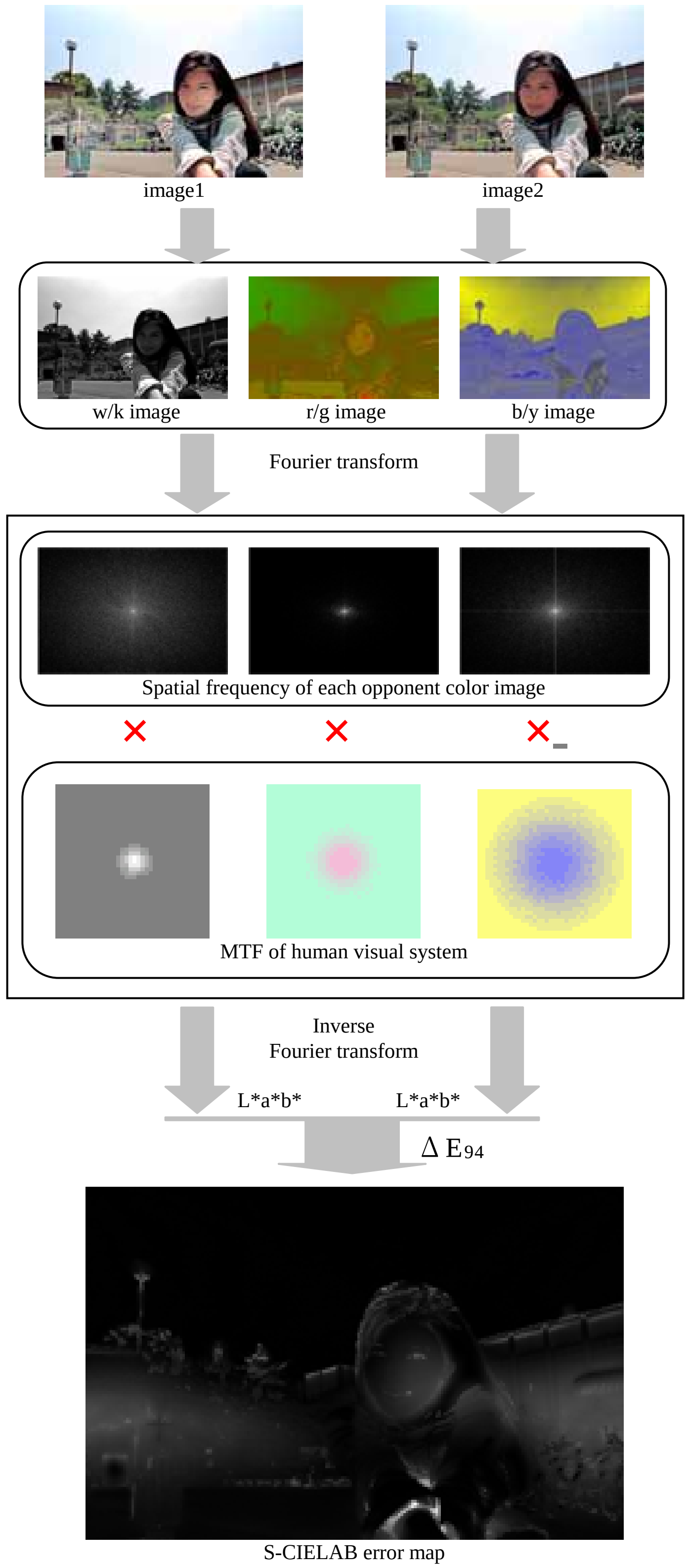

Fig.5 Flow chart of calculating S-CIELAB

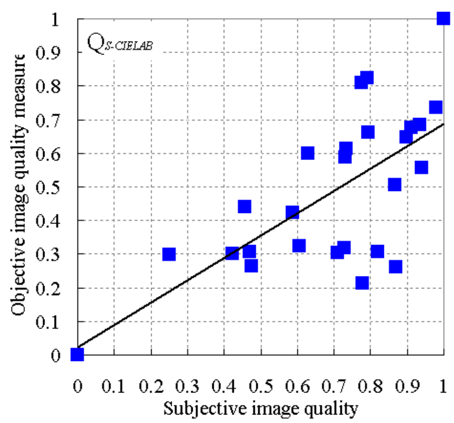

(a) Relationship between $Q_{S-CIELAB}$ and the observer rating value

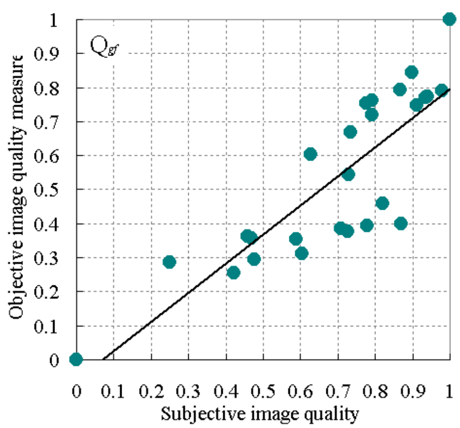

(b) Relationship between Q_{gf} and the observer rating value

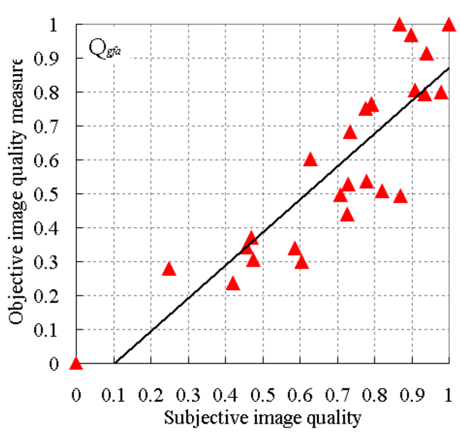

(c) Relationship between Q_{gfa} and the observer rating value

Fig.6 Relationship between the objective image quality measures and the observer rating values by using all image groups.

gazing frequency map over the whole area Q_{gf}, and the average S-CIELAB color difference weighted by the gazing frequency map only over the gazing area Q_{gfa} can be expressed by

$$Q_{gf} = \frac{\iint_{\Omega_{all}} \left(\Delta E_{S-CIELAB}(x,y) \times F(x,y)\right) dxdy}{N_p} \quad (12)$$

and

$$Q_{gfa} = \frac{\iint_{\Omega_{ga}} \left(\Delta E_{S-CIELAB}(x,y) \times F(x,y)\right) dxdy}{N_p} \quad (13)$$

where, $\Delta E_{S-CIELAB}(x,y)$ denotes the S-CIELAB color difference at each pixel. Ω_{ga} and Ω_{all} mean the gazing area and the whole area, respectively. N_p is the pixel number of image.

6. Discussions

The gazing information was introduced into the S-CIELAB metric for calculating the objective image quality. The average S-CIELAB color differences $Q_{S-CIELAB}$, the average S-CIELAB color difference weighted by the gazing frequency map over the whole area Q_{gf}, and the average S-CIELAB color difference weighted by the gazing frequency map only over the gazing area Q_{gfa} were calculated as the objective image quality measures compare to the observer rating value obtained from the subjective evaluation experiment. For the average S-CIELAB color difference weighted by the gazing frequency map only over the gazing area Q_{gfa}, the threshold was selected as 0.2.

The relationships between the normalized objective image quality measures and the normalized observer rating value of all of the images are shown in Fig.6. The correlation coefficients are 0.68, 0.84, and 0.87 respectively. It shows that the average S-CIELAB color differences with the consideration of gazing information are well correlated with the observer rating value.

7. Conclusions

In this research, we propose a new color metric based on the S-CIELAB color metric with the consideration of gazing information and discuss its effectiveness for Retinex methods. The average S-CIELAB color differences with the consideration of gazing information are well correlated with the observer rating value than $Q_{S-CIELAB}$, and the correlation coefficient of Q_{gfa} is the strongest one among them. The result shows that the frequency distribution of gazing area in the image gives most important information to evaluate the image quality.

It is verified that the proposed color metric based on S-CIELAB was effective for the evaluation of the images produced by Retinex method.

References

[1]Mark D. Fairchild, "Image Quality Measurement and Modeling for Digital Photography", *International Congress on Image Science*, pp.318-319, 2002

[2] E. H. Land, J. J. McCann: "Lightness and Retinex Theory", *J. Opt. Soc. Am*., Vol.61, pp.1-11, 1971

[3] Daniel J. Jobson, Zia-ur Rahman, and Glenn A. Woodell, "A Multiscale Retinex for Bridging the Gap Between Color Images and the Human Observation of Scenes", *IEEE Transactions on Image Processing*, Vol.6, No.7, pp.965-976, 1997

[4] CIE, Industrial Color-Difference Evaluation, *CIE Tech. Rep.* 116, Vienna, 1995

[5] Xuemei Zhang, and Brian A. Wandell, "A Spatial Extension of CIELAB for Digital Color Image Reproduc*tion", SID Journal*, pp.27-33, 1997

[6] A. L. Yarbus, Eye Movements and Vision, Plenum, 1976

[7] Kimiyoshi Miyata, Masayuki Saito, Norimichi Tsumura, Hideaki Haneishi, and Yoichi Miyake, "Eye Movement Analysis and its Application to Evaluation of Image Quality", *the Fifth Color Imaging Conference: Color Science, System, and Application*, pp.116-119, 1997

[8] C. Endo, A. Takuya, H. Haneishi, Y. Miyake, "Analysis of the eye movements and its applications to image evaluation", *Proceedings of IS&T and SID's 2nd Color Imaging Conference: Color Science, Systems and Applications*, pp.153-156, 1994

[9] N. Tsumura, C. Endo, H. Haneishi, Y. Miyake, "Image Compression and decompression based on gazing area", *Proceedings of IS&T/SPIE Symposium on Electronic Imaging 96: Human Vision and Electronic Imaging*, Vol. 2657, pp.361-367, 1996

[10] D. J. Jobson, Z. Rahman: "Properties and Performance of a Center/Surround Retinex", *IEEE Transactions on Image Processing*, Vol.6, No.3, pp.451-462, 1997

[11] Yuki Takematsu, Toshiya Nakaguchi, Norimichi Tsumura, Yoichi Miyake, " Improvement of Image Quality using Retinex Theory Based on the Statistical Image Evaluation", *Journal of The Society of Photographic Science and Technology of Japan*, Vol. 60, No.4, pp.410-416, 2004

[12] Masato Yoda, Hiroaki Kotera, "Appearance Improvement of Color Image by Adaptive Linear Retinex Model", *IS&T's NIP20: International Conference on Digital Printing Technologies*, pp. 660-663, 2004

[13] Jason S. Babcock, Jeff B. Pelz, and Mark D. Fairchild, "Eye tracking observers during color image evaluation tasks", *Proceedings of the 2003 PICS Digital Photography Conference*, pp. 218-230, Rochester, NY, 2003

[14] Handbook of Eye Tracking System EMR-8B, *Nac Image Technology Inc*.

[15] Handbook of Processing Visual Information, *the Vision Society of Japan*, 2000

Jie Bai received the B.E. degree in Thermal Energy and Power Engineering from Huazhong University of Science and Technology, Wuhan, China, in 1996 and the M.E. degree in Electronics and Mechanical Science from Chiba University, Chiba, Japan, in 2001, respectively. She is currently pursuing the Ph.D. degree in Information Science at Chiba University. Her Ph.D. dissertation focuses on image processing and image quality evaluation in consideration of the characteristics of the human eye. Her research interests include image processing, and image quality evaluation. She is a member of the Institute of Electronics, Information and Communication Engineers (IEICE), Japan and Society of Photographic Science and Technology of Japan.

Toshiya Nakaguchi received the B.E., M.E., and Ph.D. degrees from Sophia University, Tokyo, Japan in 1998, 2000, and 2003, respectively. He is currently a Research Associate in the Department of Information and Image Sciences, Chiba University, Japan. His research interests include medical engineering, color image processing, computer vision, and computer graphics. Dr. Nakaguchi is a member of the IEEE, IS&T, the Institute of Electronics, Information and Communication Engineers (IEICE), Japan and Society of Photographic Science and Technology of Japan.

Norimichi Tsumura received the B.E., M.E. and Dr. Eng degrees in Applied Physics from Osaka University in 1990, 1992 and 1995, respectively. He moved to the Department of Information and Computer Sciences, Chiba University in April 1995, as an Assistant Professor. He is currently Associate Professor in Department of Information and Image Sciences, Chiba University since February 2002. He got the Optics Prize for Young Scientists (The Optical Society of Japan) in 1995, Applied Optics Prize for the excellent research and presentation (The Japan Society of Applied Optics) in 2000, Charles E. Ives Award (Journal Award: IS&T) in 2002, 2005. He is interested in the color image processing, computer vision, computer graphics and biomedical optics.

Yoichi Miyake is the Director of the Research Center for Frontier Medical Engineering and Professor of Image Science in Chiba University. He received the Ph.D. degree from Tokyo Institute of Technology in 1978. He is a Fellow of IS&T. In 2003, he became honoree member of IS&T. In January 2000, IS&T and SPIE, named him as the Electronic Imaging Honoree of the Year. He was served as president of SPSTJ from 1999 to 2001 and as vice president of IS&T from 2000 to 2004. He was also served as guest professor of University of Rochester, USA in 1997, and Chulalongkorn University, Thailanf from 1998 to 2004. He published 20 books on the image analysis and color science.